Journal of Porous Materials (2022) 29:279–289
https://doi.org/10.1007/s10934-021-01166-1

Superhydrophobic silk fibroin-silica melamine sponge for efficient oil–water separation

Zuqin Cheng[1] · Ke Zheng[2] · Shaoqi Zhou[1,2,3,4]

Accepted: 14 October 2021 / Published online: 26 October 2021

Abstract

This study developed a facile and environmentally-friendly method to prepare SiO_2/silk fibroin (SF) composite melamine sponges modified using SF and hydrophobic SiO_2 nanoparticles (NPs). During the preparation procedure, the SiO_2 NPs were bonded to skeletons of porous sponges with the SF binding agent using a dip-coating method. The SiO_2 NPs and SF with hydrophobicity constructed a rough surface. The obtained sponges possess a high absorption capacity of 70.9–160.8 times of its weight for various oils and organic solvents and a high water-contact angle greater than 151°. More importantly, the modified sponges showed good recyclability, and could return to its original shape even after 100 cyclic compression. The as-prepared sponge also showed high buoyancy outstanding elasticity, and maintained high absorption capacity even after 10 cycles of repetitive absorption-desorption. The prepared sponges could efficiently separate oil or organic solvents from oil–water mixtures, indicating that the SiO_2/SF/MS sponges are promising candidates for remediating oil spills and oily wastewater.

Keywords Superhydrophobic/superoleophilic melamine sponge · Dip-coating approach · Silk fibroin · Hydrophobic SiO_2 nanoparticles

1 Introduction

The frequently occurring oil spills and discharge of chemical organic solvents have caused significant damage to marine ecosystems and human health and safety [1–3]. For example, the oil spill in the Gulf of Mexico released 4.9 million barrels of crude oil, covering ~ 149,000 km^2 of surface area according to the satellite images. The pollution affected human health in the near-shore water. Moreover, the perniciousness of the oils lasts for several years [4]. Therefore, many traditional oil spill remediation methods were developed, including membrane separation, [5–8] in situ combustion [9], biodegradation [10], chemical treatment [11], and mechanical removal [12]. Many drawbacks exist in traditional oil spill remediation, such as complicated fabrication processes, air pollution produced, and limited removal capacities. Absorption based on porous materials is a good alternative for oil recovery because of its low cost, fast and effective oil absorption, and high adsorption. Recently, several absorption materials have been developed, such as sponges [13–18], aerogels [19–21], biochar [22], electrospun nanofibers [23], cotton fabrics [24–26], carbon nanotubes [27], and foams [28].

Given the excellent properties of high adsorption capacity and easy oil recovery, sponges have been developed as an alternative absorbent. However, the pristine sponge is amphiphilic, restricting the separation of oil from oily water. Hence, surface modification of sponges, transferring the hydrophilic surface to hydrophobic surface, attracted much

✉ Ke Zheng
easonzk@126.com

✉ Shaoqi Zhou
fesqzhou@scut.edu.cn

1 School of Environment and Energy, Guangzhou Higher Education Mega Center, South China University of Technology, Guangzhou 510006, People's Republic of China

2 School of Civil Engineering and Transportation, South China University of Technology, Wushan, Guangzhou 510640, People's Republic of China

3 Guizhou Academy of Sciences, Shanxi Road 1, Guiyang 550001, People's Republic of China

4 State Key Laboratory of Subtropical Building Science, South China University of Technology, Guangzhou 510641, People's Republic of China

attention. The hydrophobic surface with a water-repellent property hinders water to permeate the sponge.

Many superhydrophobic materials exist in nature, such as lotus [29], water striders [30], mussels, rice leaves [31], kales [32], butterfly wings [33], and gecko setaes [34] The surface of lotus leaves is randomly distributed with convex micro- and nanostructures. The structure makes the water drop from an air barrier layer when it contacts the lotus leaf's surface. Nature-inspired hydrophobic surfaces with macro or nanostructures have been the subject of interest in the past decade. The geometrical structure and surface-free energy govern surface wettability characteristics. Many studies have reported on constructing superhydrophobic surfaces by combining a rough structure with a low energy surface. Li et al. [35] fabricated a superhydrophobic/superoleophilic sponge using a core-shell fluorinated-polyacrylate latex and hydrophobic SiO_2 NPs. The as-prepared sponge has a high water-contact angle (WCA) of 150.5° and is maintained above 140° after abrading using sandpaper for 10 cycles. The coated sponge had a faster oil absorption rate than the pristine sponge. Mi et al. [36] synthesized a superhydrophobic fluorinated fibrous silica sponge by crosslinking and fluorination using glutaraldehyde and perliuorodecyltrieth-oxysilane. The obtained sponge had a high WCA of 151°, high oil absorption capacities of ~ 122 times its weight, and excellent separation efficiency of 98% after five cycles of selective absorption. Guselnikova et al. [37] reported on a superhydrophobic/superoleophilic polyurethane sponge with 3,5-bis(trifluoromethyl)benzenediazonium tosylate. The as-prepared sponge had an extremely high WCA of 160 ± 1°, with an absorption capacity of 35–77 times its weight, and excellent separation efficiency (over 99.9% for emulsion). The fluorinated compounds were used in many hydrophobic materials because of their low surface energy. However, the fluorinated compounds are non-biodegradable and could bioaccumulate in the environment, which is concerning to the environment and human life when absorbents are used in oil spill remediation. Therefore, it is challenging to fabricate environmentally-friendly oil absorbent materials.

Up to now, various methods have been reported for preparing superhydrophobic sponges, such as layer-by-layer assembly, dip-coating, chemical vapor deposition, spray coating, electrospinning, and etching. Among these methods, the dip-coating method was a facile preparation. To prepare superhydrophobic surfaces, rough structures were the most common by incorporating nanosized particles, such as TiO_2 [5, 38], SiO_2 [14, 39], ZnO [40], and Fe_3O_4 [41, 42], on the skeletons of the materials. SiO_2 was a common modification material for constructing hydrophobic surfaces. Yao et al. [43] proposed a superhydrophobicity bio-based polybenzoxazine/SiO_2-modified fabric for oil/water separation. The obtained fabrics had high oil fluxes of 6500–9500 L/(m^2·h) and strong durability in harsh environments. Ge et al. [44] developed a superhydrophobic polyurethane (PU) sponge for oil/water separation by coating with SiO_2 nanoparticles (NPs). The sponge exhibited high elasticity, high oil absorption capacity, and excellent recyclability.

We construct a rough surface of porous melamine sponge by coating the surface with hydrophobic SiO_2 NPs to obtain a superhydrophobic/superoleophilic oil absorbent material. A problem in the sponge modification process is that the hydrophobic SiO_2 NPs is weakly adhered to the surface of the sponge and easily peeled off. We present silk fibroin (SF) as a binder, which originated from *Bombyx mori* silk. *Bombyx mori* silk is composed of SF and silk sericin (SS). Sericin could be easily removed from *Bombyx mori* silk by boiling it in Na_2CO_3 water [45]. SF predominantly consists of glycine, alanine, serine, tyrosine, and valine, with ratios of 45.9%, 30.3%, 12.1%, 5.3%, and 1.8%, respectively [46]. SF has a light chain (~ 390 kDa) and a heavy chain (~ 26 kDa). A single disulfide bridge linked the light and heavy chains [47–49]. The heavy chain contains a hydrophobic region, consisting of a highly duplicated hexapeptide amino acid sequence (Gly-Ala-Gly-Ala-Gly-Ser) and a highly duplicated dipeptide amino acid sequence (Gly-Ala/Ser/Tyr). Gly and Ala amino acid sequences were hydrophobic. Silk secondary structures include metastable silk I and stable silk II. Silk II has an antiparallel β-sheet structure and confers insolubility in water. Silk I can form silk II by high temperature, sonication, and chemical solvents, such as methyl alcohol or potassium phosphate [50, 51].

SF is a multifunctional biomaterial because of its high mechanical strength, outstanding biocompatibility, nontoxicity, and biodegradability [48]. Because of these performances, SF has been widely used in wound healing [52, 53], hydrogel [54], aerogel [55], membrane [56], sponge [57], and scaffold [58]. Chen et al. [59] fabricated a porous scaffold to promote osteochondral repair using biocompatible and biodegradable SF. Wang et al. [60] developed a silk film for information security. The obtained film had excellent mechanical strength, long-term structural stability, and a unique response mechanism. The film shows excellent potential in carrying optical information. Zhou et al. [57] fabricated a hydrophobic silk fibroin-graphene oxide functionalized melamine sponge for oil/water separation. SF is a natural polymer to combine graphene oxide with a melamine sponge.

In this work, we propose a facile route to fabricate a superhydrophobic functionalized melamine sponge using a simple dip-coating method. SF and hydrophobic SiO_2 NPs were introduced to form a rough nanoscopic morphology on the skeletons of melamine sponge. To prepare the superhydrophobic melamine sponge, SF was used as a binder to adhere the hydrophobic SiO_2 to the skeletons of melamine sponge. A combination of the hydrophobic region in SF with the roughness of the NPs reinforced the

hydrophobicity. The functionalization process was performed using a one-step coating of hydrophobic SiO_2 NPs coated to the surface of the melamine sponge, and SF as a binder combined the melamine sponge with hydrophobic SiO_2 NPs. The process was reacted at room temperature without additional equipment, directly achieving a superhydrophobic surface without further organic hydrophobic modifications. For the hydrophobization of melamine sponge, this approach is more cost-effective and simpler than in previous reports. The obtained sponge exhibited superhydrophobicity, with a WCA exceeding 150°, separating the oil and water mixtures quickly and effectively, exhibiting excellent mechanical properties, and excellent recyclability. PDMS solution.

2 Experimental methods

2.1 Materials

MF sponge without oil/water selectivity (water contact value of 0°, *n*-hexane contact value of 0°) was used as raw material, and was purchased from a local store. *Bombyx mori* cocoons were obtained from Hangzhou Jiuyuan Silk Culture Co. Ltd, sodium carbonate anhydrous (99.8%) was bought from Fuchen (Tianjin) Chemical Reagent Co. Ltd, dodecane (98%) and LiBr (99%) was supplied by Shanghai Macklin Biochemical Co. Ltd, and hydrophobic SiO_2 NPs (7–40 nm of diameter, 260 m^2/g, hydrophobicity originated from alkylation treatment), 1,1,2,2-tetrachloroethane (TTCE, 98%), and *N*,*N*-dimethylformamide (DMF, ≥ 99.5%) were supplied by Shanghai Aladdin Biochemical Technology Co. Ltd. *n*-Hexane (≥ 97.0%) was obtained from Guangdong Guanghua Sci-Tech Co. Ltd, pump oil was supplied by Zhejiang Feiyue Electromechanical Co. Ltd, corn oil was obtained from Shenzhen Lam Soon Edible Oil Co. Ltd, and isopropyl alcohol (99.7%) was bought from Guangzhou Chemical Reagent Factory.

2.2 Preparation of SF extraction

Bombyx mori cocoons were boiled in a 0.02 M sodium carbonate aqueous solution for 30 min under constant stirring. The boiled cocoons were washed with deionized (DI) water repeatedly to remove sericin, followed by vacuum drying at 60 °C for 12 h. For preparing SF solution, 2 g degummed silk was dissolved in 100 mL 9.3 M LiBr at 80 °C for 2 h under constant stirring. After cooling to 25±2 °C, the solution was dialyzed to remove impurity ions and diluted to 0.4 mg/mL.

2.3 Preparation of SiO_2/SF/MS

A series of SF/SiO_2 solutions with different SiO_2 concentrations (0, 0.1 wt%, 0.2 wt%, 0.3 wt%, 0.4 wt%, 0.5 wt%, and 0.6 wt%) were prepared. 2 mL SF solution was mixture with 1 mL $CaCl_2$ mixture solution($CaCl_2$:C_2H_5OH:H_2O molar ratio 1:2:8), SiO_2/SF/MS were prepared by dispersing the hydrophobic SiO_2 NPs of different weights into 40 mL SF/$CaCl_2$ aqueous solution (0.4 mg/mL) under sonication at 25 ± 2 °C for 30 min. The raw melamine sponge was cut into 1 cm^3 (1 cm × 1 cm × 1 cm) pieces, followed by washing with DI and ethanol water, respectively. The washed sponge was spin-dried at 1500 rpm for 3 min and vacuum dried at 60 °C for 6 h. The sponge pieces were immersed in the SF/SiO_2 solution for 24 h under continuous shaking. The sponge pieces were spin-dried at 1500 rpm for 3 min to remove the residual solution, then washed with ethanol three times. Lastly, the sponge pieces were vacuum dried at 60 °C for 6 h. SiO_2/SF/MS was obtained. Unless otherwise specified, the composite SiO_2/SF/MS used for characterization and oil adsorption measurement was SiO_2/SF/MS with the SiO_2 content of 0.3 wt%.

2.4 Characterization

The surface morphology of the sponge was analyzed using a high-resolution field emission (FE) scanning electron microscope (SEM) (FE-SEM, Merlin, Zeiss, Germany). Fourier transform infrared (FTIR) spectra were characterized using FTIR spectroscopy (Nicolet IS50 - Nicolet Continuum). For further structural analysis, thermogravimetric analysis (TGA) was observed using a simultaneous thermal analyzer (STA 449 C, Netzsch, Germany) at 25–1000 °C at a ramp rate of 10 °C/min under nitrogen atmosphere.

2.5 Surface wettability measurements

To evaluate the surface wettability of the materials, the WCA of all sponge sample surfaces was measured using a contact angle measuring system (OCA15, KRUSS, Germany). Five tests were measured at random locations on each sample using 2 μL water droplets. The final WCA results were averaged within each sponge.

2.6 Mechanical properties

The mechanical properties of the sponge were conducted using a dynamic mechanical analyzer (DMA Q800, TA, USA) to obtain the compressive stress–strain curves. The

samples were on a cyclic compression-desorption process for 100 cycles, with a fixed strain of 70% to evaluate its long-term recoverability.

2.7 Measurement of oil absorption capacity

To evaluate the oil-capturing ability, the SiO_2/SF/MS (taking 0.3 wt% as an example) was immersed in *n*-hexane, dodecane, isopropyl alcohol, pump oil, corn oil, DMF, and TTCE. In detail, a weighed small piece of SiO_2/SF/MS was placed into the oils or organic solvents for 30 s until saturated. The residual oil was removed by holding the sponge in the air for 30 s. Then, the saturated mass of the sponge was instantaneously measured. The mass absorption capacity (Q) was evaluated using the equation

$$Q = \frac{m_t - m_i}{m_i},$$

where Q represents the oil absorption capacity (g/g) of SiO_2/SF/MS, m_t (g) represents the weight of the sponge after absorption, and m_i (g) represents the weight of the sponge before adsorption.

2.8 Measurement of reusability

The reusability of the modified sponge for oils and organic solvents were evaluated using a repeated absorption-desorption test for 10 cycles. The sponge was weighed immediately after being immersed in oils or organic solvents for 30 s and holding for 30 s. The saturated sponges were spin-dried at 1500 rpm for 3 min to remove the absorbed oils or organic solvents. The absorption-desorption procedures were repeated 10 times. For each adsorption-desorption cycle, the weight of the as-prepared sponge before and after absorption was recorded to measure its absorption capacity.

3 Results and discussion

3.1 The effect of SiO_2 concentrations on SiO_2/SF/MS

The hydrophobicity of the sponge surface and absorption capacity were used to evaluate the optimum concentration of SiO_2 NPs. To obtain the optimal superhydrophobic sponge, the effect of SiO_2 concentrations on the wettability of SiO_2/SF/MS was investigated. The wettability of the materials was evaluated using the WCA, and the high WCA corresponds to high hydrophobicity [61]. Figure 1a demonstrates that the WCA of the sponge increased with the increment of consistence of SiO_2, and the WCA reached 151.9° at 0.3 wt% SiO_2. The superhydrophobic surface is defined by WCA ($\theta > 150°$); therefore, the SiO_2/SF/MS exhibits superhydrophobicity at a SiO_2 content of 0.3 wt%. The absorption capacity of each concentration was evaluated and recorded. As shown in Fig. 1b, the absorption capacity of *n*-hexane and TTCE increased first and decreased with the increment of the SiO_2 concentration and reached a maximum at the SiO_2 concentration of 0.3 wt%. Considering both aspects, the optimal concentration of SiO_2 would be at 0.3 wt%.

3.2 Characterization of SiO_2/SF/MS

3.2.1 Morphology of SiO_2/SF/MS

The surface morphology of the pristine melamine sponge and SiO_2/SF/MS with different concentrations of SiO_2 were characterized using FE-SEM (Fig. 2). Note that the pristine melamine sponge displays a three-dimensional open-cell structure with pore sizes ranging from 100 to 180 μm, vital for possessing a high oil absorption capacity for absorbent materials. The higher magnification images of the pristine sponge show that the skeletons were smooth and bead-free

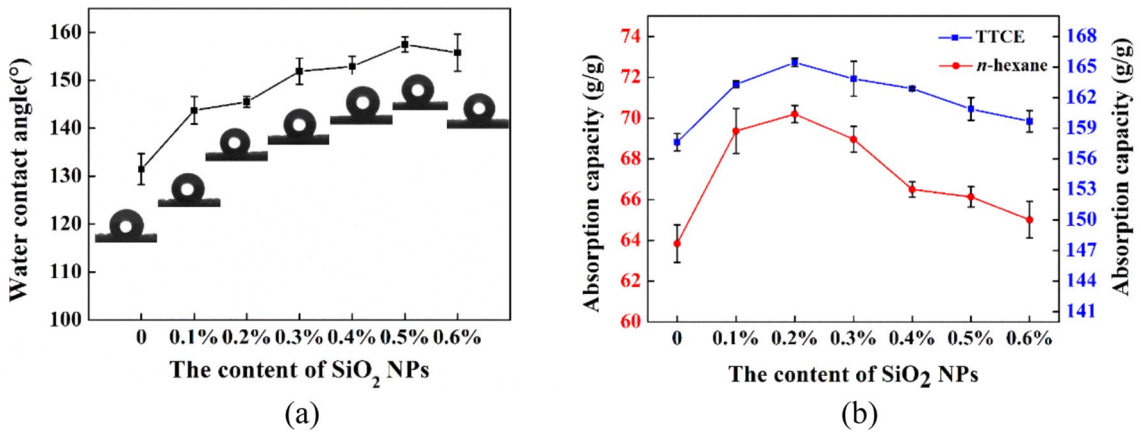

Fig. 1 The water contact angle (**a**) and absorption capacity for *n*-hexane and TTCE (**b**) of SiO_2/SF/MS with different SiO_2 content (Color figure online)

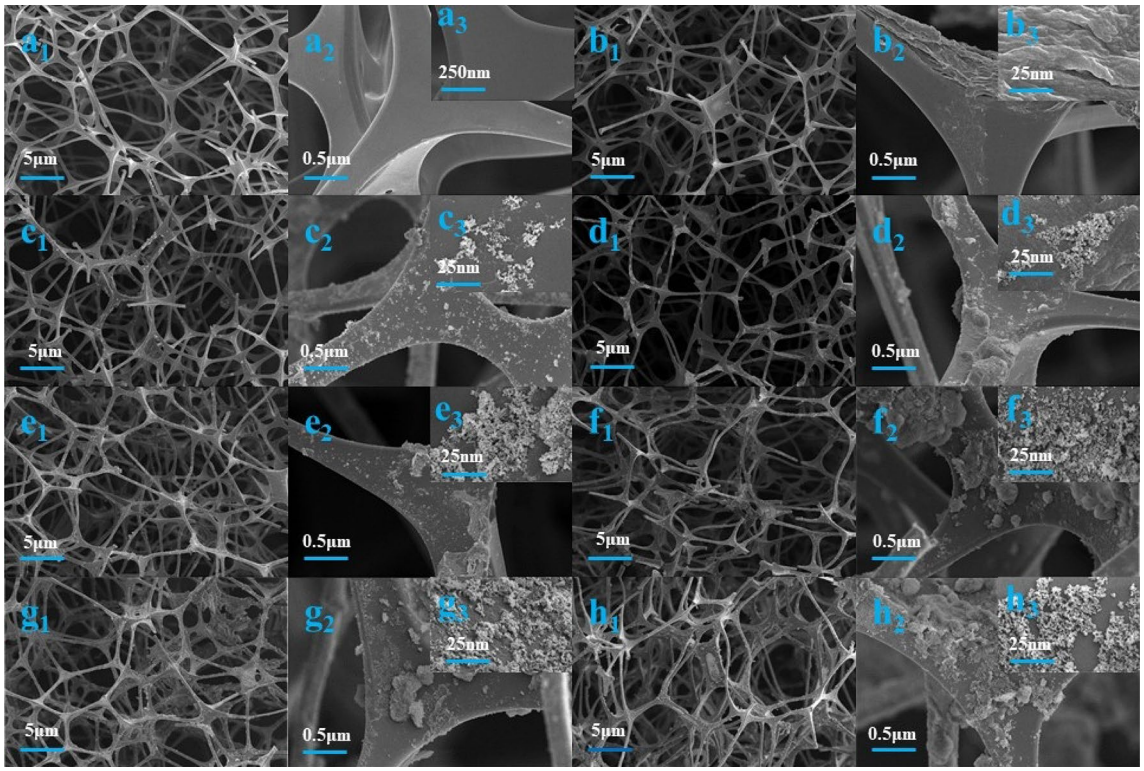

Fig. 2 The photographs of **a** MS, **b** SF/MS, **c** 0.1% SiO_2/SF/MS, **d** 0.2% SiO_2/SF/MS, **e** 0.3% SiO_2/SF/MS, **f** 0.4% SiO_2/SF/MS, **g** 0.5% SiO_2/SF/MS, and **h** 0.6%SiO_2/SF/MS

(Fig. 2a_1–a_3). After immersion in the SF solution, the original open-cell structure was retained, SF flocs were generated on the surface of the sponge skeletons (Fig. 2b_1–b_3), leading to rough skeletons. Furthermore, the nanoscale dimension particles were adhered to the backbones of the sponges after adding hydrophobic SiO_2 NPs. From Fig. 2c–h, more particles loaded on the junction points, attributed to the increasing SiO_2 content. At the high SiO_2 concentration, numerous NPs aggregated into different size balls, enhancing the surface roughness as necessary. These images confirm that SF and hydrophobic SiO_2 NPs were attached to the surface and interior of the sponge successfully. Therefore, the melamine sponge was transformed from a hydrophilic to superhydrophobic sponge.

3.2.2 FTIR analysis of SiO_2/SF/MS

To verify the presence of hydrophobic SiO_2 NPs, FTIR spectra of MS, SF/MS SiO_2/SF/MS, SF, and hydrophobic SiO_2 NPs were analyzed and compared (Fig. 3). Strong absorption peaks occurred at 3330, 1540, 1159, and 810 cm^{-1} related to secondary amine (N–H), C=N stretching, C–O stretching vibration, and triazine ring bending vibration, all observed in MS, SF/MS, and SiO_2/SF/MS. Furthermore, absorption peaks at 1333 and 980 cm^{-1} linked to C–H bending also

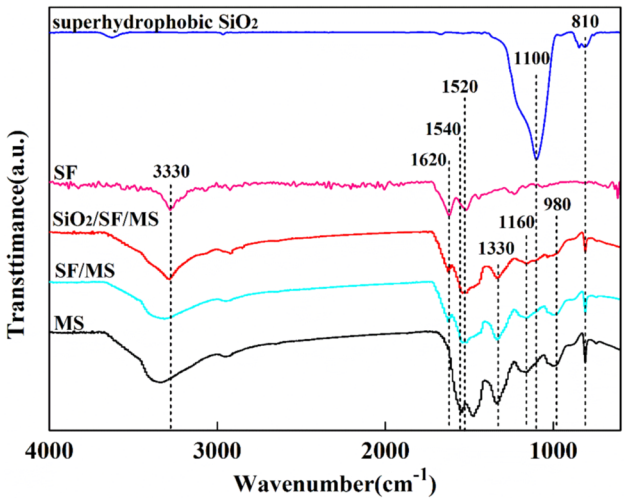

Fig. 3 The FTIR spectra of MS, SF/MS, SiO_2/SF/MS, SF, and superhydrophobic SiO_2 NPs

appeared in pure and modified sponges. SF predominantly consists of three conformation states: random coils, α-helix (silk I), and β-sheets (silk II). The SF secondary structures could be confirmed by the characteristic bands corresponding to amide I and amide II [62]. From the FTIR spectra of

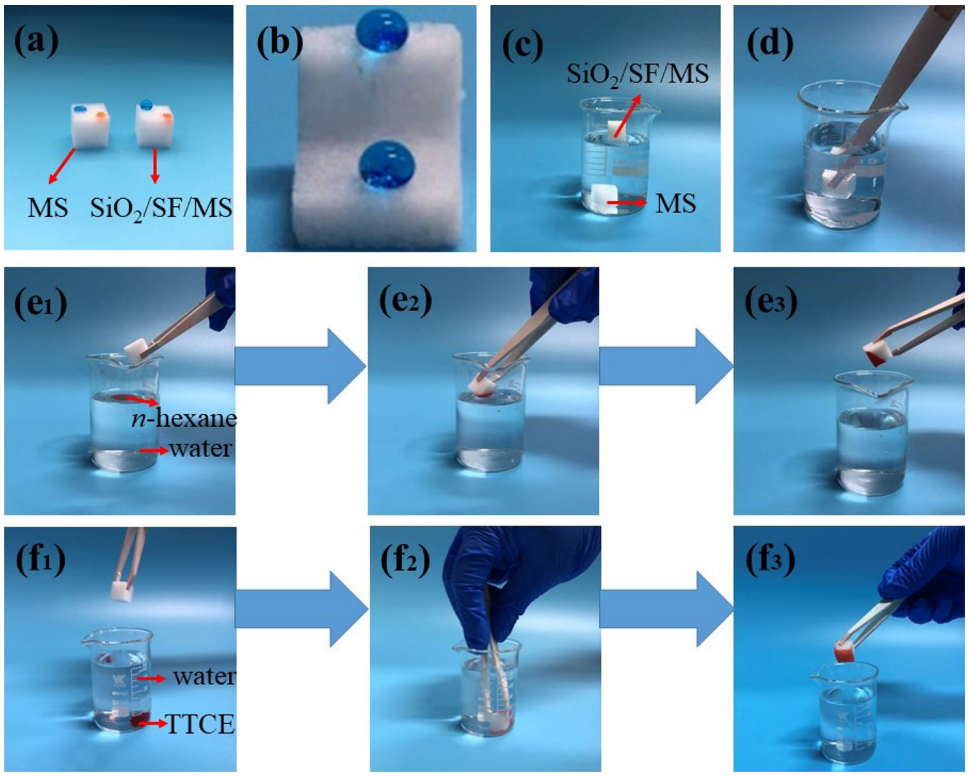

Fig. 4 **a** Water (dyed blue) and *n*-hexane droplets (dyed red) dropped onto the surface of MF, and SiO_2/SF/MS. **b** The water droplet wetting behaviors on the the surface and section of the SiO_2/SF/MS. **c** The images of the MS and SiO_2/SF/MS after placing it on the water surface. **d** Water immersion images of SiO_2/SF/MS by external force. The images of the absorption process of **e1**-**e3** light oil (*n*-hexane), (f1-f3) heavy oil (TTCE) (Color figure online)

SF, SF/MS, and SiO_2/SF/MS, the strong absorption peaks at 1625 cm^{-1} and 1521 cm^{-1} were ascribed to the stretching vibrations of amide I and amide II, corresponding to the Silk II conformation (β-sheet). Furthermore, the absorption peak at 2964 cm^{-1} in the spectrum of the SiO_2 NPs was ascribed to $–CH_3$ antisymmetric stretching vibration, which provides the SiO_2 NPs hydrophobicity. Besides, strong absorption peaks at 1100 cm^{-1} and 810 cm^{-1} shown in the hydrophobic SiO_2 NPs and SiO_2/SF/MS spectra were ascribed to Si–O–Si antisymmetric and symmetric stretching vibrations, indicating that the melamine sponge was successfully modified using hydrophobic SiO_2 NPs.

3.2.3 Wettability property

The specific wettability is a critical consideration for the absorbent in applying the treatment of oil spill accidents. The pristine and modified sponges, with mass SiO_2 concentrations of 0.3 wt%, exhibited different wettability. To better visualize the wetting performance of pristine melamine and modified sponges, we dyed water with methylene blue and *n*-hexane with sudan III. Figure 4a shows that water and *n*-hexane droplets could penetrate the pristine melamine sponge quickly and entirely, leaving a blue and red circle contact area. However, the *n*-hexane droplet permeated into SiO_2/SF/MS immediately, whereas the water droplet maintained a spherical shape, indicating that the air in the sponge was replaced by *n*-hexane. Figure 1a shows that the WCA of SiO_2/SF/MS (0.3 wt%) is 151.9°. Furthermore, the water droplet on the interior of the modified sponge also maintained a spherical shape (Fig. 4b), verifying superhydrophobicity and superoleophobicity of the surface and interior of the SiO_2/SF/MS.

When placed into water, the pure melamine sponge imbibed water immediately and sank to the bottom of the beaker (Fig. 4c), whereas the SiO_2/SF/MS could continuously float on the water surface and without sinking. When an external force was applied to the SiO_2/SF/MS (Fig. 4d), the sponge was immersed in the water, with a silver mirror-like surface, attributing to the air bubble layer trapped between water and superhydrophobic melamine sponge, preventing the water from entering the interior.

The three-dimensional porous structure and superhydrophobicity of the sponge make it a promising candidate absorbent for efficient oil/water separation. The porous structure creates a high absorbance for oils, and the superhydrophobicity endows excellent water repellency. To confirm the selective absorption performance of SiO_2/SF/MS, *n*-hexane and TTCE were chosen as light oil and heavy oil samples, respectively. For better visualization of the separation process, *n*-hexane and TTCE were dyed with sudan III. As shown in Fig. $4e_1$–e_3 and f_1–f_3, when the SiO_2/SF/MS is placed on the water with *n*-hexane dispersing on the water surface, the sponge absorbed the oil immediately and floated on the water surface because of its water repellency. No oil droplets are left on the remaining liquid surface after

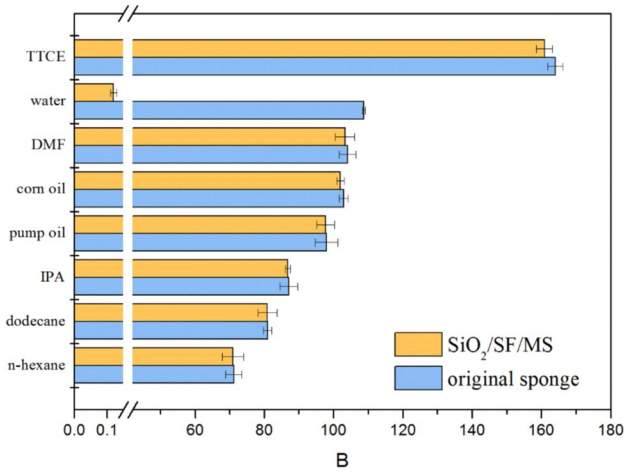

Fig. 5 Absorption capacity of or original sponge and SiO_2/SF/MS with SiO_2 concentration of 0.3 wt% for different oils and organic solvents

removing the sponge. Similarly, when the SiO_2/SF/MS was placed into water to absorb TTCE at the bottom of the beaker, the sponge quickly absorbed TTCE, and no residual oil droplets were observed after removing the sponge from the water.

3.2.4 Absorption capacity of SiO_2/SF/MS

To assess the absorption capacity of SiO_2/SF/MS, absorption experiments were conducted on various oils and organic solvents, including hydrocarbon solvent (*n*-hexane and dodecane), halogenated hydrocarbon (TTCE), alcohol solvents (isopropyl alcohol), oils (pump oil and corn oil), DMF, and water.

From Fig. 5, the absorption capacities of the original sponge and SiO_2/SF/MS for different oils and organic solvents were almost the same, but the water absorption capacities showed significant difference. However, the water absorption capacity of original sponge was 108.7 g/g, while that of the SiO_2/SF/MS was only 0.12 g/g. The hydrophilic modification didn't affect the absorption capacities of sponge for the oils and organic solvents, but made the sponge own oil/water selectivity. The absorption capacities of the SiO_2/SF/MS, for *n*-hexane, dodecane, isopropyl alcohol, pump oil, corn oil, DMF, and TTCE were 70.9, 80.9, 86.8, 97.7, 102.0, 103.3, and 160.8 g/g, respectively. Especially, the absorption capacity for TTCE reached 160.8 times its weight. The differences in the results because of the density, viscosity, and surface tension values of the oils and solvents [63, 64], show that the absorption capacity is proportionate to the oil or organic solvents' density. For instance, TTCE has the highest density among these liquids, and the absorption capacity is higher than others by absorbing the same volume. The density of *n*-hexane is the lowest, and the absorption capacity is relatively less. The *n*-hexane is the one of most widely used chemical to evaluate the adsorption capability. So the *n*-hexane absorption capacity was used to compare the performance with the other researches, the results were shown in Table 1. The *n*-hexane absorption capacity of SiO_2/SF/MS in this work are better than most of the reported sponge materials. Moreover, the as-prepared SiO_2/SF/MS sponge possessed unique merits, including low density, high buoyancy, and low fabrication cost, making it a promising oil absorbent for oil/water mixture remediation.

3.2.5 Reusability and stability

For oil absorbents, two vital parameters should be considered. One is the absorption capacity, and another is reusability because of economic and ecological demands. The prepared melamine sponge was used to absorb *n*-hexane for 30 cycles. Saturated organic solvents were removed using a centrifugal dehydrator. Figure 6 shows the variation of absorption capacity of SiO_2/SF/MS for *n*-hexane during 30 repetitive absorption-desorption cycles. The results showed that the modified sponge performed stable oil absorption

Table 1 Comparsion of modification methods, absorption capacity and WCA of other sponge absorbents reported in literature

Sponge absorbents	Modification method	*n*-Hexane absorption capacity(g/g)	WCA (°)	References
LMF	Deposition	58	135	[13]
EPOP-1@PU sponge	Condensation	48	154.5	[15]
PDA/PDVB/sponge	One-pot	24	141	[16]
Fe_3O_4/HDPE PU sponge	Dip-coating	15	155	[41]
PU/PDA/HMDS	Dip-coating	21	153	[43]
TA/octadecylamine/MS	One-pot	68	154.8	[65]
SiO_2/SF/MS	Dip-coating	70.9	151.9	This work

LMF lignin/melamine-formaldehyde sponge, *EPOP-1@PU sponge* ether-based porous organic polymer-1/ polyurethane sponge, *PDA/PDVB/sponge* polydopamine/polydivinylbenzene/sponge, *Fe_3O_4/HDPE PU sponge* Fe_3O_4/high-density polyethylene/ polyurethane sponge, *TA/Octadecylamine/MS*: tannic acid/Octadecylamine/melamine sponge, *PU/PDA/HMDS* polyurethane sponge/polydopamine/hexamethyl disilazane

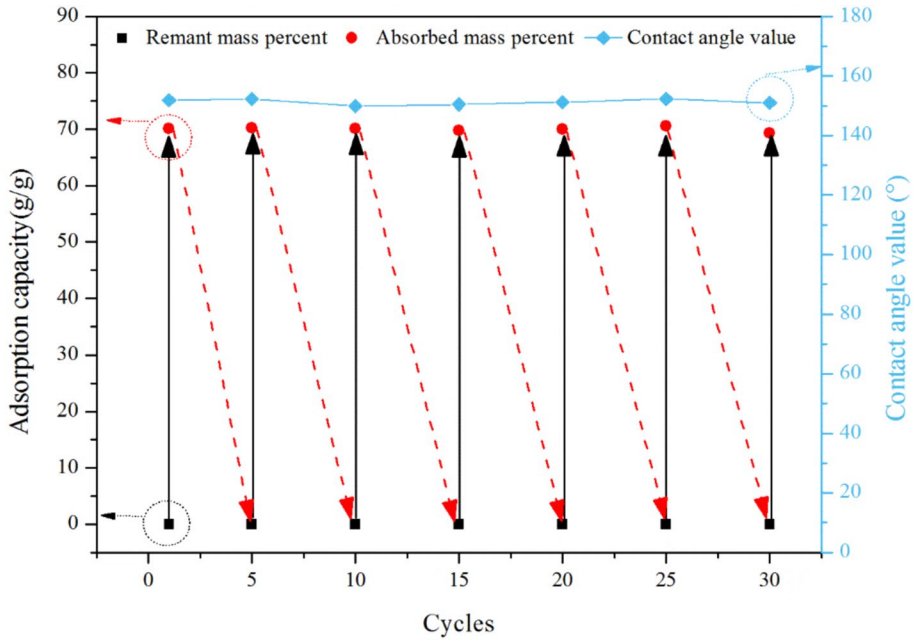

Fig. 6 Recyclability of SiO_2/SF/MS over 30 absorption-desorption cycles for adsorption and contact angle value

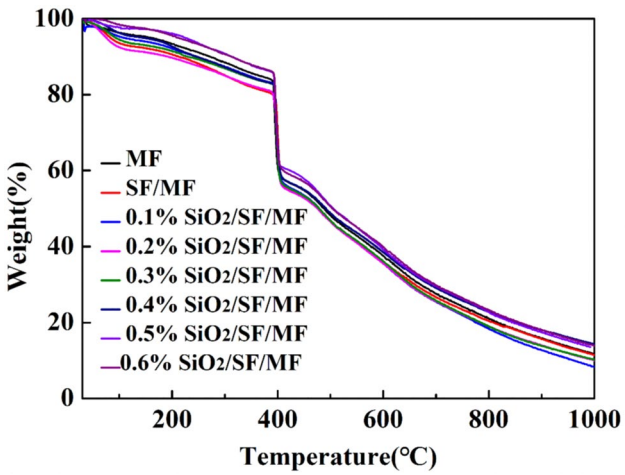

Fig. 7 TGA curves of MF and SiO_2/SF/MS

capacity and contact value. In details, the decrease of oil absorption capacity was less than 4%, and the contact angle value was still above 150° after 30 cycles. Hence, the modified sponge achieved admirable stability and durability.

3.2.6 Simultaneous thermal analysis (STA)

STA was used to confirm the attachment of silica and SF on the sponge skeleton surface, revealing the composition thermal stability of the neat MF and SiO_2/SF/MS. From Fig. 7, all samples exhibited similar thermogravimetric curves, demonstrating that the addition of the SF and hydrophobic SiO_2 NPs did not change the thermal degradation mechanism of the melamine sponge. This was ascribed to the low SF and hydrophobic SiO_2 NPs concentrations that did not alter the principal compositions of the melamine sponge. The first weight loss (~10 wt%) under 120 °C was caused by water evaporation. The second weight loss, in the range of 120–360 °C, was attributed to eliminate formaldehyde from the ether bridge to form methylene bridges. The primary weight loss between 380 and 400 °C is linked to the breakdown of methylene bridges of melamine sponge. The final weight loss between 400 and 1000 °C of all samples was ascribed to the thermal decomposition of the triazine ring. Although all sample curves exhibited similar thermal behavior, the residual weight of uncoated MF (12.28%) was lower than that of SiO_2/SF/MS at the SiO_2 content between 0.4 wt% and 0.6 wt% after being heated to 1000 °C. The residual mass of SiO_2/SF/MS (at 0–0.1 wt% SiO_2) was lower than the pure melamine sponge and decreased with increasing SiO_2 concentration. The reason could be that at the low SiO_2 content, the SF adhered to the sponge. The results demonstrated that the thermal stability of the sponge was enhanced after modification using enough hydrophobic SiO_2 NPs.

3.2.7 Mechanical properties

Mechanical performance is a significant parameter for superwetting materials in oil/water mixture separation, which is vital for sustainable reuse and operation flexibility. The stress–strain curves of the modified sponge were obtained from a repeated 100-times compression-releasing process with a maximum strain of 70%. Even after 100 cycles, the pure melamine sponge with a 3D porous structure exhibits its excellent elasticity and flexibility, making it an excellent template for preparing oil absorbent. The method we

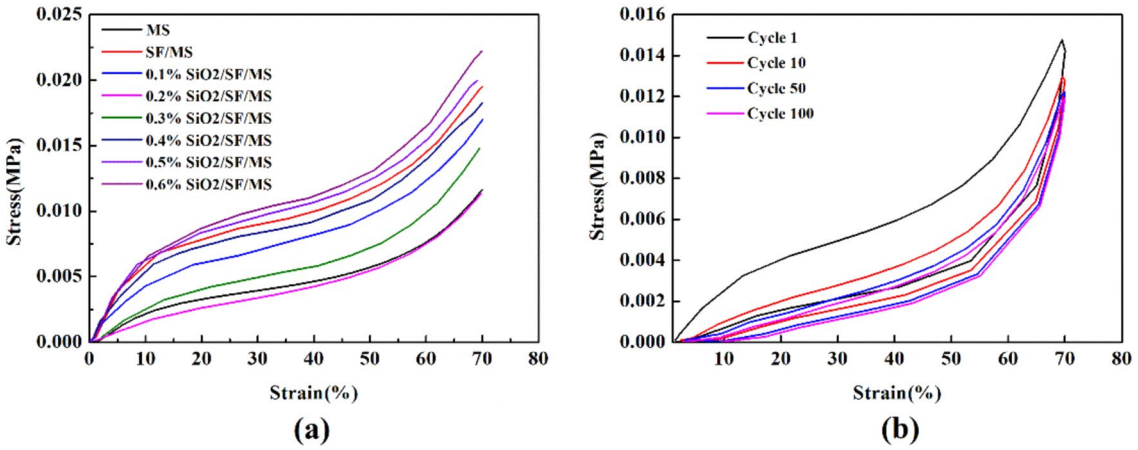

Fig. 8 The compressive stress–strain curves of **a** MF and SiO_2/SF/MS with different hydrophobic SiO_2 NPs concentration and **b** cyclic stress–strain curves of SiO_2/SF/MS at 70% strain for 100 cycles

adopted did not damage the structure of the pristine melamine sponge. To investigate the mechanical behaviors of pristine melamine sponge and SiO_2/SF/MS (taking 3 wt% as an example), compressive stress versus strain curves in a strain-range from 0 to 70% were obtained from consecutive cyclic compression and release tests (Fig. 8). From the compressive stress–strain curves, the compressive stress at 70% strain of SF/MS was 0.0195 MPa, which is higher than 0.011 MPa of pure melamine sponge, indicating that SF addition reinforced its compressive stress, which could be attributed to its unique mechanical strength on SF. Furthermore, with increasing hydrophobic SiO_2 NPs, the stresses declined first and increased at hydrophobic SiO_2 NPs concentrations of 0.3 wt%, indicating that adding high SiO_2 concentrations reinforced its compressive stress. Furthermore, the sponge regained its original shape and is highly elastic with no obvious fractures even after 100 cycles when the stress was released. This could be observed from the curves returning to pristine points after releasing the force, which demonstrated its excellent elasticity and flexibility. The outstanding mechanical property of SiO_2/SF/MS makes it a reusable oil absorbent in oily water remediation.

4 Conclusions

We have fabricated a novel and environmentally-friendly superhydrophobic/superoleophilic SiO_2/SF/MS as an absorbing material using a simple dip-coating approach with SF and hydrophobic SiO_2 NPs. The eco-friendly SF functioned as a binder, which coated the melamine sponge backbone with hydrophobic SiO_2 NPs and transformed the smooth backbones into roughness, and consequently, in superhydrophobicity and superoleophobicity. The fabricated superhydrophobic and superoleophilic melamine sponge was founded on the principles of constructing roughness on the surface of the skeletons to enhance its wettability property. This was realized by introducing hydrophobic SiO_2 NPs onto the surface of the skeletons by SF solution coating. The hydrophobic SiO_2 NPs enhanced the roughness of the skeletons, endowed the melamine sponge hydrophobicity, and increased its affinity with oil. The SiO_2/SF/MS exhibited a high WCA of 151.9°. The modified melamine sponge showed excellent oil-absorbing ability and excellent heat-resistance ability. Our findings demonstrated that the commercial melamine sponge could be successfully transferred into high-efficient high-viscosity oil absorbents using simple modification, which is beneficial to alleviate the increasing oil spillage problems and provide a feasible route to reuse the waste melamine sponge.

Acknowledgements Financial support from the Ministry of Science and Technology of China for the National Key Research and Development Program of China (Grant No. 2016YFC0400702-6) is gratefully acknowledged.

References

1. M.G. Barron, Ecological impacts of the deepwater horizon oil spill: implications for immunotoxicity. Toxicol. Pathol. **40**(2), 315–320 (2012)
2. A.J. Howarth, M.J. Katz, T.C. Wang, A.E. Platero-Prats, K.W. Chapman, J.T. Hupp, O.K. Farha, High efficiency adsorption and removal of selenate and selenite from water using metal-organic frameworks. J. Am. Chem. Soc. **137** (23), 7488–7494 (2015)
3. E. Kintisch, An audacious decision in crisis gets cautious praise. Science **329**(5993), 735–73 (2010)
4. I.R. MacDonald, O. Garcia-Pineda, A. Beet, S. Daneshgar Asl, L. Feng, G. Graettinger, D. French-McCay, J. Holmes, C. Hu, F. Huffer, I. Leifer, F. Muller-Karger, A. Solow, M. Silva, G. Swayze, Natural and unnatural oil slicks in the Gulf of Mexico. J. Geophys. Res. Oceans **120**(12), 8364–8380 (2015)

5. Y. Kang, S. Jiao, B. Wang, X. Lv, W. Wang, W. Yin, Z. Zhang, Q. Zhang, Y. Tan, G. Pang, PVDF-modified TiO_2 nanowires membrane with underliquid dual superlyophobic property for switchable separation of oil–water emulsions. ACS Appl. Mater. Interfaces **12**(36), 40925–4093 (2020)
6. X. Yue, J. Li, T. Zhang, F. Qiu, D. Yang, M. Xue, In situ one-step fabrication of durable superhydrophobic-superoleophilic cellulose/LDH membrane with hierarchical structure for efficiency oil/water separation. Chem. Eng. J. **328**, 117–123 (2017)
7. M. Zhang, W. Ma, S. Wu, G. Tang, J. Cui, Q. Zhang, F. Chen, R. Xiong, C. Huang, Electrospun frogspawn structured membrane for gravity-driven oil–water separation. J. Colloid Interface Sci. **547**, 136–144 (2019)
8. K. Wang, X. Liu, Y. Tan, W. Zhang, S. Zhang, J. Li, Two-dimensional membrane and three-dimensional bulk aerogel materials via top-down wood nanotechnology for multibehavioral and reusable oil/water separation. Chem. Eng. J. **371**, 769–780 (2019)
9. J. Aurell, B.K. Gullett, Aerostat sampling of PCDD/PCDF emissions from the Gulf oil spill in situ burn. Environ. Sci. Technol. **44**(24), 9431–9437 (2010)
10. R. Boopathy, S. Shields, S. Nunna, Biodegradation of crude oil from the BP oil spill in the marsh sediments of southeast Louisiana. USA. Appl. Biochem. Biotechnol. **167**(6), 1560–1568 (2012)
11. E.B. Kujawinski, M.C. Kido Soule, D.L. Valentine, A.K. Boysen, K. Longnecker, M.C. Redmond, Fate of dispersants associated with the deepwater horizon oil spill. Environ. Sci. Technol. **45**(4), 1298–1306 (2011)
12. J. Ge, Q. Jin, D. Zong, J. Yu, B. Ding, Biomimetic multilayer nanofibrous membranes with elaborated superwettability for effective purification of emulsified oily wastewater. ACS Appl. Mater. Interfaces **10**(18), 16183–16192 (2018)
13. H. Yu, W. Zhan, Y. Liu, Engineering lignin nanoparticles deposition on melamine sponge skeleton for absorbent and flame retardant materials. Waste Biomass Valoriz. **11**(8), 4561–4569 (2019)
14. R. Zhang, Z. Zhou, W. Ge, Y. Lu, T. Liu, W. Yang, J. Dai, Robust, fluorine-free and superhydrophobic composite melamine sponge modified with dual silanized SiO_2 microspheres for oil–water separation. Chin. J. Chem. Eng. **33**, 50–60 (2020)
15. Y. Tang, H. Huang, X. Guo, C. Zhong, Superhydrophobic ether-based porous organic polymer-coated polyurethane sponge for highly efficient oil–water separation. Ind. Eng. Chem. Res. **59**(29), 13228–13238 (2020)
16. J. Xie, J. Zhang, X. Zhang, Z. Guo, Y. Hu, Durable multifunctional superhydrophobic sponge for oil/water separation and adsorption of volatile organic compounds. Res. Chem. Intermed. **46**(9), 4297–4309 (2020)
17. X. Shi, Y. Lan, S. Peng, Y. Wang, J. Ma, Green fabrication of a multifunctional sponge as an absorbent for highly efficient and ultrafast oil–water separation. ACS Omega **5**(24), 14232–14241 (2020)
18. K. Yin, D. Lu, B. Sun, T. Kalwarczyk, R. Holyst, J. Hao, H. Li, J. Hao, Photoluminescent, ferromagnetic, and hydrophobic sponges for oil–water separation. ACS Omega **5**(25), 15077–15082 (2020)
19. H. Zhang, J. Zhang, The preparation of novel polyvinyl alcohol (PVA)-based nanoparticle/carbon nanotubes (PNP/CNTs) aerogel for solvents adsorption application. J. Colloid Interface Sci. **569**, 254–266 (2020)
20. X.-L. Wu, T. Wen, H.-L. Guo, S. Yang, X. Wang, A.-W. Xu, Biomass-derived sponge-like carbonaceous hydrogels and aerogels for supercapacitors. ACS Nano **7**(4), 3589–3597 (2013)
21. N. Cao, Q. Lyu, J. Li, Y. Wang, B. Yang, S. Szunerits, R. Boukherroub, Facile synthesis of fluorinated polydopamine/chitosan/reduced graphene oxide composite aerogel for efficient oil/water separation. Chem. Eng. J. **326**, 17–28 (2017)
22. X. Huang, Y. Jiang, R. Yu, Popped rice biochar and superhydrophobic SiO_2/popped rice biochar for oil adsorption. Silicon **13**, 2661–2669 (2020)
23. B. Zaarour, L. Zhu, X. Jin, Direct fabrication of electrospun branched nanofibers with tiny diameters for oil absorption. J. Dispers. Sci. Technol. **100**, 100 (2020). https://doi.org/10.1080/01932691.2020.1798779
24. X. Yan, X. Zhu, Y. Ruan, T. Xing, G. Chen, C. Zhou, Biomimetic, dopamine-modified superhydrophobic cotton fabric for oil–water separation. Cellulose **27**(13), 7873–7885 (2020)
25. A.S. Belal, M.M.A. Khalil, M. Soliman, S. Ebrahim, Novel superhydrophobic surface of cotton fabrics for removing oil or organic solvents from contaminated water. Cellulose **27**(13), 7703–7719 (2020)
26. J. Li, X. Wu, P. Jiang, L. Li, J. He, W. Xu, W. Li, A facile method to fabricate durable super-hydrophobic cotton fabric. J. Vinyl Addit. Technol. **26**(1), 3–9 (2019)
27. W. Wang, Y. Li, Y. Feng, J. Han, F. Zhang, P. Long, C. Peng, C. Cao, Y. Cao, H. Yang, W. Feng, Asymmetric self-supporting hybrid fluorinated carbon nanotubes/carbon nanotubes sponge electrode for high-performance lithium-polysulfide battery. Chem. Eng. J. **349**, 756–765 (2018)
28. M. Anju, N.K. Renuka, Magnetically actuated graphene coated polyurethane foam as potential sorbent for oils and organics. Arab. J. Chem. **13**(1), 1752–1762 (2020)
29. S. Wang, Y. Zhu, F. Xia, J. Xi, N. Wang, L. Feng, L. Jiang, The preparation of a superhydrophilic carbon film from a superhydrophobic lotus leaf. Carbon **44**(9), 1848–1850 (2006)
30. X. Gao, L. Jiang, Water-repellent legs of water striders. Nature **432**, 36 (2004)
31. L. Jiang, S.K.L.M.C.F. Donghua Univ, M. Polymer, *Superhydrophobic surfaces: From natural to artificial* (Chemical Industry Press, Beijing, 2005), pp. 58–59
32. E. Alizadeh-Birjandi, H.P. Kavehpour, Plant leaves icephobicity. J. Coat. Technol. Res. **14**(5), 1061–1067 (2017)
33. Y. Zheng, X. Gao, L. Jiang, Directional adhesion of superhydrophobic butterfly wings. Soft Matter **3**(2), 178–182 (2007)
34. K. Autumn, M. Sitti, Y.A. Liang, A.M. Peattie, W.R. Hansen, S. Sponberg, T.W. Kenny, R. Fearing, J.N. Israelachvili, R.J. Full, Evidence for van der Waals adhesion in gecko setae. Proc Natl Acad Sci U S A **99**(19), 12252–12256 (2002)
35. K. Li, X. Zeng, H. Li, X. Lai, Facile fabrication of a robust superhydrophobic/superoleophilic sponge for selective oil absorption from oily water. RSC Adv. **4**, 45 (2014)
36. H.-Y. Mi, H. Li, X. Jing, Q. Zhang, P.-Y. Feng, P. He, Y. Liu, Robust superhydrophobic fluorinated fibrous silica sponge with fire retardancy for selective oil absorption in harsh environment. Sep. Purif. Technol. **241**, 116700 (2020)
37. O. Guselnikova, A. Barras, A. Addad, E. Sviridova, S. Szunerits, P. Postnikov, R. Boukherroub, Magnetic polyurethane sponge for efficient oil adsorption and separation of oil from oil-in-water emulsions. Sep. Purif. Technol. **240**(2020)
38. J. Ren, F. Tao, L. Liu, X. Wang, Y. Cui, A novel TiO_2@stearic acid/chitosan coating with reversible wettability for controllable oil/water and emulsions separation. Carbohydr. Polym. **232**, 115807 (2020)
39. M. Li, C. Bian, G. Yang, X. Qiang, Facile fabrication of water-based and non-fluorinated superhydrophobic sponge for efficient separation of immiscible oil/water mixture and water-in-oil emulsion. Chem. Eng. J. **368**, 350–358 (2019)
40. J.-M. Yi, D. Wang, F. Schwarz, J. Zhong, A. Chimeh, A. Korte, J. Zhan, P. Schaaf, E. Runge, C. Lienau, Doubly resonant plasmonic hot spot–exciton coupling enhances second harmonic generation from Au/ZnO hybrid porous nanosponges. ACS Photonics **6**(11), 2779–2787 (2019)

41. T. Yu, F. Halouane, D. Mathias, A. Barras, Z. Wang, A. Lv, S. Lu, W. Xu, D. Meziane, N. Tiercelin, S. Szunerits, R. Boukherroub, Preparation of magnetic, superhydrophobic/superoleophilic polyurethane sponge: separation of oil/water mixture and demulsification. Chem. Eng. J. **384**(2020)
42. Z. Yin, Y. Li, T. Song, M. Bao, Y. Li, J. Lu, Y. Li, An environmentally benign approach to prepare superhydrophobic magnetic melamine sponge for effective oil/water separation. Sep. Purif. Technol. **236,** 123339 (2020)
43. H. Yao, X. Lu, Z. Xin, H. Zhang, X. Li, A durable bio-based polybenzoxazine/SiO_2 modified fabric with superhydrophobicity and superoleophilicity for oil/water separation. Sep. Purif. Technol. **229**, 116308 (2019)
44. B. Ge, X. Men, X. Zhu, Z. Zhang, A superhydrophobic monolithic material with tunable wettability for oil and water separation. J. Mater. Sci. **50**(6), 2365–2369 (2015)
45. G.H. Altman, R.L. Horan, H.H. Lu, J. Moreau, I. Martin, J.C. Richmond, D.L. Kaplan, Silk matrix for tissue engineered anterior cruciate ligaments. Biomaterials **23**(20), 4131–4141 (2002)
46. C.Z. Zhou, F. Confalonieri, M. Jacquet, R. Perasso, Z.G. Li, J. Janin, Silk fibroin structural implications of a remarkable amino acid sequence. Proteins **44**(2), 119–122 (2001)
47. C. Vepari, D.L. Kaplan, Silk as a biomaterial. Prog. Polym. Sci. **32**(8-9), 991–1007 (2007)
48. D.N. Rockwood, R.C. Preda, T. Yucel, X. Wang, M.L. Lovett, D.L. Kaplan, Materials fabrication from Bombyx mori silk fibroin. Nat Protoc **6**(10), 1612–1631 (2011)
49. H.-J. Jin, D.L. Kaplan, Mechanism of silk processing in insects and spiders. Nature **424**(6952):1057–1061 (2003)
50. L.F. Drummy, D.M. Phillips, M.O. Stone, B.L. Farmer, R.R. Naik, Thermally induced alpha-helix to beta-sheet transition in regenerated silk fibers and films. Biomacromolecules **6**(6), 3328–3333 (2005)
51. K. Numata, P. Cebe, D.L. Kaplan, Mechanism of enzymatic degradation of beta-sheet crystals. Biomaterials **31**(10), 2926–2933 (2010)
52. U.Y. Karatepe, T. Ozdemir, Improving mechanical and antibacterial properties of PMMA via polyblend electrospinning with silk fibroin and polyethyleneimine towards dental applications. Bioact. Mater. **5**(3), 510–515 (2020)
53. Y. Zhang, L. Lu, Y. Chen, J. Wang, Y. Chen, C. Mao, M. Yang, Polydopamine modification of silk fibroin membranes significantly promotes their wound healing effect. Biomater. Sci. **7**(12), 5232–5237 (2019)
54. W. Liu, Y. Sun, X. Dong, Q. Yin, H. Zhu, S. Li, J. Zhou, C. Wang, Cell-derived extracellular matrix-coated silk fibroin scaffold for cardiogenesis of brown adipose stem cells through modulation of TGF-beta pathway. Regen. Biomater. **7**(4), 403–412 (2020)
55. H. Maleki, L. Whitmore, N. Husing, Novel multifunctional polymethylsilsesquioxane-silk fibroin aerogel hybrids for environmental and thermal insulation applications. J. Mater. Chem. A Mater. **6**(26), 12598–12612 (2018)
56. W. Chen, F. Li, L. Chen, Y. Zhang, T. Zhang, T. Wang, Fast self-assembly of microporous silk fibroin membranes on liquid surface. Int. J. Biol. Macromol. **156**, 633–639 (2020)
57. J. Zhou, Y. Zhang, Y. Yang, Z. Chen, G. Jia, L. Zhang, Silk fibroin-graphene oxide functionalized melamine sponge for efficient oil absorption and oil/water separation. Appl. Surf. Sci. **497**, 143762 (2019)
58. T. Ni, M. Liu, Y. Zhang, Y. Cao, R. Pei, 3D bioprinting of bone marrow mesenchymal stem cell-laden silk fibroin double network scaffolds for cartilage tissue repair. Bioconjug. Chem. **31**(8), 1938–1947 (2020)
59. A. Reizabal, C.M. Costa, P.G. Saiz, B. Gonzalez, L. Perez-Alvarez, R. de FernandezLuis, A. Garcia, J.L. Vilas-Vilela, S. Lanceros-Mendez, Processing strategies to obtain highly porous silk fibroin structures with tailored microstructure and molecular characteristics and their applicability in water remediation. J. Hazard. Mater. **403**, 123675 (2021)
60. Z. Wang, F. Meng, S. Zhang, Y. Meng, S. Wu, B. Tang, Robust, portable, and specific water-response silk film with noniridescent pattern encryption for information security. ACS Appl. Mater. Interfaces **12**(50), 56413–56423 (2020)
61. D. Quéré, Wetting and roughness. Annu. Rev. Mater. Res. **38**(1), 71–99 (2008)
62. X. Hu, D. Kaplan, P. Cebe, Determining beta-sheet crystallinity in fibrous proteins by thermal analysis and infrared spectroscopy. Macromolecules **39**(18), 6161–6170 (2006)
63. X. Wang, Y. Lu, C.J. Carmalt, I.P. Parkin, X. Zhang, Multifunctional porous and magnetic silicone with high elasticity, durability, and oil–water separation properties. Langmuir **34**(44), 13305–13311 (2018)
64. S. Qiu, Y. Li, G. Li, Z. Zhang, Y. Li, T. Wu, Robust superhydrophobic sepiolite-coated polyurethane sponge for highly efficient and recyclable oil absorption. ACS Sustain. Chem. Eng. **7**(5), 5560–5567 (2019)
65. N. Zhang, Y. Zhou, Y. Zhang, W. Jiang, T. Wang, J. Fu, Dual-templating synthesis of compressible and superhydrophobic spongy polystyrene for oil capture. Chem. Eng. J. **354**, 245–253 (2018)